



# Investigation on the Collapse Mechanism of Overlying Clay Layer Based on the Unified Strength Theory

Fan Chen<sup>a</sup>, Yingchao Wang<sup>a,b</sup>, Yuanhai Li<sup>a</sup>, and Wen Jiang<sup>c</sup>

<sup>a</sup>State Key Laboratory for Geomechanics and Deep Underground Engineering, China University of Mining & Technology, Xuzhou 221116, China

<sup>b</sup>State Key Laboratory of Geomechanics and Geotechnical Engineering, Institute of Rock and Soil Mechanics, Chinese Academy of Sciences, Wuhan 430071, China

<sup>c</sup>School of Mechanics & Civil Engineering, China University of Mining & Technology, Xuzhou 221116, China

## ARTICLE HISTORY

Received 18 October 2021  
Revised 6 March 2022  
Accepted 15 March 2022  
Published Online 1 July 2022

## KEYWORDS

Water and sand gushing  
Ground collapse  
Unified strength theory  
Critical cavity radius  
Cavity

## ABSTRACT

Water and sand gushing will lead to the destruction of upper cohesive soil that further form cavity, and the ground collapse caused by the development of soil cavity adversely affects the geotechnical building or foundation. In this study, the theory of elastic mechanics clamped beam was used to establish the arbitrary point stress calculation model and the stress solution of the clay soil under the action of gravity was derived. According to the equilibrium state of ultimate stress and unified strength theory, the formula for calculating the critical radius of cavity induced by water and sand gushing was obtained. The parametric study of above formulas shows that the cavity radius decreases with the increased depth of clay layer and Poisson's number of clay layer. The higher the clay cohesion is, the higher is the cavity clay. Moreover, the limit radius of cavity first increases and then decreases with the increased of clay thickness. The results of theoretical analysis of critical collapse radius and the results of model test demonstrate that the calculating value of critical collapse radius based on unified strength theory is consistent with the test results.

## 1. Introduction

With the vigorous development of underground infrastructure, water and sand leakage will inevitably occur in the process of underground construction such as seepage erosion of underground pipelines, water and sand leakage of tunnel lining and runoff of karst water (Korff et al., 2011; Yang et al., 2018; Chen et al., 2021). In the process of water and sand leakage, a cave forms up and gradually expands under the clay after particles migration. When the stress at a certain point in the clay exceeds its ultimate strength, the clay would collapse in blocks. It would cause land subsidence and even more serious would cause land collapse, which produce significant economic losses and seriously endanger human security. Therefore, it is of great significance to study the failure mechanism and critical conditions of clay soil induced by water and sand leakage.

Aiming at the critical conditions of soil seepage failure, many scholars have carried out a lot of researches and achieved some

valuable results. Kenney and Lau (1985), Indratna et al. (2011) and Mao (2005) have put forward the evaluation method of soil internal stability from soil geometric conditions, which has been verified by a large number of theoretical, experimental and engineering practices. Indraratna and Vafai (1997) have proposed a theoretical model of fine particles migration along pore channels based on the concept of equivalent aperture. Huang et al. (2017) have established a theoretical model to predict the critical hydraulic gradients for soil particle movement using sediment particle rolling theory. Li and Fannin (2012) have obtained the calculation formula for hydraulic gradient of seepage failure by taking the zero effective stress state of fine particles as the seepage failure condition of soil. Israr and Indraratna (2019) have modeled the critical hydraulic gradient of soil seepage failure by considering the effects of antiparticle and boundary frictions and stress reduction in the soil. Wang and Li (2020) have established formula for calculating the starting critical hydraulic gradient of sandy soil fine particle during the suffusion process according to

**CORRESPONDENCE** Fan Chen ✉ 1228586533@qq.com 📧 State Key Laboratory for Geomechanics and Deep Underground Engineering, China University of Mining & Technology, Xuzhou 221116, China

© 2022 Korean Society of Civil Engineers

the equilibrium state of ultimate stress by considering the effective stress of soil and the reduction of fine particle stress. However, the current researches mainly focus on the migration process of fine particles and hydraulic gradient of seepage failure in sandy soil. The non-cohesive soil gets too much attention from scholars while there is relatively few studies on the seepage failure mechanism of clay.

Aiming at the clay collapse caused by water and sand leakage, combined with the elasticity theory, this paper establishes the force model of clay collapse from the perspective of ultimate bearing capacity. And then, the calculation formula of critical cavity radius for clay collapse is deduced, which provides a quantitative analysis basis for the study of clay collapse. We also study the variation law of the critical cavity radius with the depth, Poisson's ratio, cohesion of clay layer. The indoor experimental results and the existing model tests indicate that the calculation formula can accurately predict the critical cavity radius for clay collapse.

## 2. Failure Mechanism of Clay

As shown in Fig. 1, the upper part is clay and the lower part is sandy soil. The sand particles loss due to the seepage erosion of underground pipelines, water and sand leakage of tunnel lining, runoff of karst water, which would form cavity between the sandy soil layer and the cohesive soil layer (Fig. 1(a)). The cavity is small in the initial stage, so the clay could remain stable because the cohesive soil has certain cohesion and strong self-stability ability. With the continuous occurrence of water and sand leakage, the cavity is expanding, and the clay blocks around the cavity collapse and accumulate at the bottom of the cavity (Fig. 1(b)). The soil cave formed by the clay blocks collapse continue developing to the surface, which eventually leads to ground collapse by inducing factors triggered (Fig. 1(d)). If the thickness of soil layer is enough, a pressure arch would be

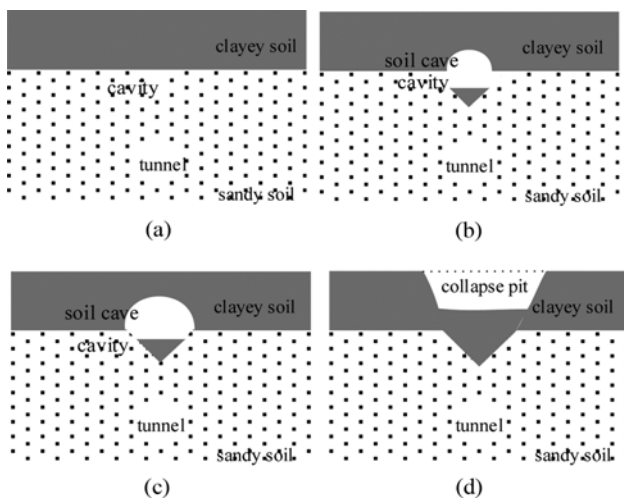


Fig. 1. Clay Blocks Collapse Caused by Sand Leakage: (a) Cavity Formed, (b) Clay Blocks Collapse, (c) Pressure Arch Formed, (d) Ground Collapse



Fig. 2. Road Collapse Accident in Xining City

formed when the soil cave expands to a certain height (Fig. 1(c)). When the arching effect fails due to great changes in external conditions, the upper cohesive soil collapses and forms a collapse pit.

For example, on January 13, 2020, the road collapse accident occurred in Xining, Qinghai, China, due to cavity formed caused by soil loss, as shown in Fig. 2. The water seepage of collapsible loess roadbed for many years led to the loss of subgrade soil gradually. The external cavity of dilapidated buried shelter provided channel for soil erosion, and then the underground cave formed. Under the repeated action of regular load, the original design capacity of subgrade busted and the bearing capacity declined, which caused the road collapse and further drive the bus falling and breaking the water supply pipeline, a large amount of tap water leaked out and finally resulted in a large-area collapse.

## 3. Mechanical Criterion of Clay Collapse in Cavity Evolution

### 3.1 Stress Calculation of Clay Layer considering Gravity

According to the above cases, clay collapse can be simplified to the model shown in Fig. 3. The failure of clayey soil mainly depends on the thickness of soil layer and its own ultimate bearing capacity. Because there are soil supporting around the cavity, the clay floor could be regarded as the clamped boundary. The top of the clamped beam model is subjected to the soil gravity above the clay and its self-weight. It is assumed that the model meets the elasticity calculation conditions. Assuming that

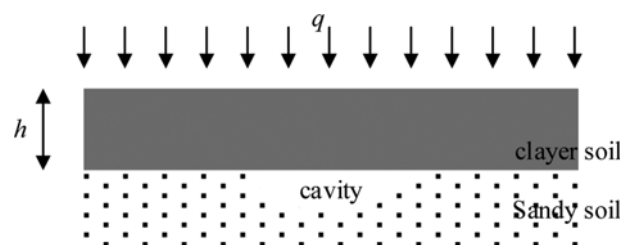


Fig. 3. Critical Collapse Model of Clay Block

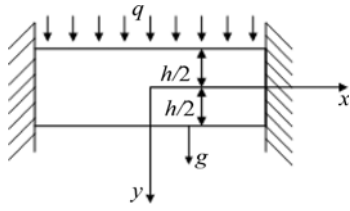


Fig. 4. Analysis Diagram of Clamped Beam

the radius of the cavity is  $l$ , the stress at the bottom of the clayey layer shown in Fig. 4 is deduced according to the elastic theory.

As shown in Fig. 4, the thickness of clay layer is  $h$ , the length of cavity is  $2l$ , The Rankine soil pressure of the overlying clay is  $q$ , and the unit width is taken for analysis. According to the two-dimensional elastic equilibrium equation (Xu, 2006), the stress function of each point in clay can be obtained as follows:

$$\begin{cases} \sigma_x = \frac{1}{2}x^2(6Ay + 2B) - 2Ay^3 - 2By^2 + 6Hy + 2K \\ \sigma_y = Ay^3 + By^2 + Cy + D - \rho gy \\ \tau_{xy} = -3Axy^2 - 2Bxy - Cx. \end{cases} \quad (1)$$

The main boundary conditions on the upper and lower sides are

$$(\sigma_y)_{y=\pm\frac{h}{2}} = -q, (\sigma_y)_{y=\pm\frac{h}{2}} = 0, (\tau_{xy})_{y=\pm\frac{h}{2}} = 0. \quad (2)$$

By solving Eqs. (1) and (2), Eq. (3) can be obtained:

$$\begin{cases} \sigma_x = -\frac{6(q + \rho gh)}{h^3}x^2y + \frac{4(q + \rho gh)}{h^3}y^3 + 6Hy + 2K \\ \sigma_y = -\frac{2(q + \rho gh)}{h^3}y^3 + \frac{3q + \rho gh}{2h}y - \frac{q}{2} \\ \tau_{xy} = \frac{6(q + \rho gh)}{h^3}xy^2 - \frac{3(q + \rho gh)}{2h}x. \end{cases} \quad (3)$$

According to geometric and physical equations, Eq. (4) can be obtained:

$$\begin{cases} u = \frac{1}{E} \left( -\frac{2(q + \rho gh)}{h^3}x^3y + \frac{4(q + \rho gh)}{h^3}xy^3 + 6Hxy + 2Kx \right) + \\ \frac{\mu}{E} \left( \frac{2(q + \rho gh)}{h^3}xy^3 - \frac{3q + \rho gh}{2h}xy + \frac{q}{2}x \right) - wy + u_0 \\ v = \frac{\mu}{E} \left( \frac{3(q + \rho gh)}{h^3}x^2y^2 - \frac{(q + \rho gh)}{h^3}y^4 - 3Hy^2 - 2Ky \right) + \\ \frac{1}{E} \left( -\frac{(q + \rho gh)}{2h^3}y^4 + \frac{3q + \rho gh}{4h}y^2 - \frac{q}{2}y \right) + wx + v_0 - \\ \frac{1}{E} \left( 3Hx^2 + \frac{\mu(3q + 5\rho gh)}{4h}x^2 - \frac{(q + \rho gh)}{2h^3}x^4 + \frac{3(q + \rho gh)}{2h}x^2 \right), \end{cases} \quad (4)$$

where  $u_0$ ,  $v_0$  and  $w$  are constants representing rigid displacement. According to the symmetry,  $u$  is an odd function of  $x$  and  $v$  is an even function of  $x$ , so it could be obtained that  $u_0 = 0$ ,  $w = 0$ .

Since the displacement at both ends of clamped beam remain unchanged, the following boundary conditions can be obtained (Ding et al., 2005; Zhong and Yu, 2007):

$$\text{Point } (l, 0), u = v = 0, \frac{\partial u}{\partial y} = 0. \quad (5)$$

By substituting Eqs. (4) and (5), Eq. (6) can be obtained:

$$\begin{cases} H = \frac{q + \rho gh}{3h^3}l^2 + \frac{\mu(3q + \rho gh)}{12h} \\ K = \frac{\mu q}{4} \\ v_0 = \frac{1}{E} \left( \frac{(q + \rho gh)}{2h^3}l^4 + \frac{6(\mu + 1)(q + \rho gh)}{12h} \right). \end{cases} \quad (6)$$

Substituting the calculated coefficient into Eq. (3), the stress component is

$$\begin{cases} \sigma_x = -\frac{6(q + \rho gh)}{h^3}x^2y + \frac{4(q + \rho gh)}{h^3}y^3 + \\ \left( \frac{2(q + \rho gh)}{h^3}l^2 + \frac{\mu(3q + \rho gh)}{2h} \right) y - \frac{\mu q}{2} \\ \sigma_y = -\frac{2(q + \rho gh)}{h^3}y^3 + \frac{3q + \rho gh}{2h}y - \frac{q}{2} \\ \tau_{xy} = \frac{6(q + \rho gh)}{h^3}xy^2 - \frac{3(q + \rho gh)}{2h}x. \end{cases} \quad (7)$$

### 3.2 Relevant Formulas Derivation Based on Unified Strength Theory

The stress state of geotechnical materials in nature is complex, the simplified model is used for analysis in most cases. Since Mohr Coulomb's strength theory was put forward, international scholars have put forward hundreds of yield criteria for materials with equal tensile and compressive strength and failure theories for materials with different tensile and compressive strength, but these theories can only apply to specific materials (Yu et al., 2020). The unified strength theory can be flexibly applied to different materials, and considers all stress components acting on the double shear element and different effects on material failure. It is more widely used in geotechnical engineering (Wu et al., 2020).

The unified strength theory expressed by normal stress and geotechnical materials can be expressed as (Yu et al., 2020)

$$\begin{cases} F = \frac{1}{1+b}(\sigma_1 + b\sigma_2) - \frac{1 - \sin\phi_0}{1 + \sin\phi_0}\sigma_3 = \frac{2c_0 \cos\phi_0}{1 + \sin\phi_0} \\ \sigma_2 \geq \frac{1}{2}(\sigma_1 + \sigma_3) - \frac{\sin\phi_0}{2}(\sigma_1 - \sigma_3) \\ b = \frac{2(\sin\phi_{UST} - \sin\phi_0)}{2\sin\phi_0 - (1 + \sin\phi_0)\sin\phi_{UST}}, \end{cases} \quad (8)$$

where  $c_0$  is cohesion,  $\phi_0$  is the internal friction angle,  $\phi_{UST}$  is the uniform internal friction angle,  $b$  is the Unified strength theory parameters.

If the intermediate principal stress parameter  $m$  is introduced,

make  $\sigma_2 = m/2(\sigma_1 + \sigma_3)$ , Eq. (8) becomes

$$F = \frac{2+bm}{2(1+b)}\sigma_1 - \frac{(1-\sin\phi_0)(1+2b-bm)}{2(1+b)(1+\sin\phi_0)}\sigma_3 = \frac{2c_0\cos\phi_0}{1+\sin\phi_0} \quad (9)$$

When the soil is in elastic state,  $m < 1$ ; When the soil yield,  $m \rightarrow 1$

When  $m = 1$ , Eq. (9) is simplified as

$$F = \frac{2+b}{2(1+b)}\sigma_1 - \frac{(1-\sin\phi_0)(2+b)}{2(1+b)(1+\sin\phi_0)}\sigma_3 = \frac{2c_0\cos\phi_0}{1+\sin\phi_0} \quad (10)$$

### 3.3 Critical Radius of Cavity in Clay Collapse

According to Eq. (7), the normal stress and shear stress under the soil are 0, and the tensile stress reaches the maximum at  $(0, h/2)$ , then the principal stress under the soil is

$$\sigma_1 = ((q + \rho gh)(4l^2 + 2h^2 + \mu h^2))/4h^2 \quad \sigma_3 = 0 \quad (11)$$

By substituting  $\sigma_1, \sigma_3$  into Eq. (10), it can be obtained that the critical radius of cavity in clay soil instability is

$$l = \sqrt{\frac{2c_0\cos\phi_0(1+b)h^2}{(1+\sin\phi_0)(2+b)(q+\rho gh)} - \frac{(2+\mu)}{4}h^2} \quad (12)$$

The relationship between sand inflow and cavity radius is

(Zheng et al., 2016):

$$l = \sqrt{2H\left(\frac{\beta S}{\pi}\right)^{1/2} (1-\varepsilon^2)^{3/4} - H^2(1-\varepsilon^2)}, \quad (13)$$

where  $H$  is the distance between leakage point and cavity,  $S$  is the amount of sand inflow,  $\varepsilon$  is the elliptical eccentricity.

Then the critical sand inflow can be obtain:

$$\left(\frac{\beta S}{\pi}\right)^{1/2} = \frac{8c_0\cos\phi_0(1+b) - (2+\mu)(1+\sin\phi_0)(2+b)(q+\rho gh)}{8H(1+\sin\phi_0)(2+b)(1-\varepsilon^2)^{3/4}(q+\rho gh)} h^2 + \frac{H(1-\varepsilon^2)^{1/4}}{2} \quad (14)$$

According to the above formula, we can predict clay collapse after the sand leakage in underground pipelines or tunnel lining. And then reduce the suddenness of ground collapse disaster and win time for taking preventive measures and take preventive measures in time.

### 4. Parameter Analysis of Cavity Critical Radius

According to the above deducing progress, the clayey soil stability is related to parameters such as depth, Poisson's ratio,

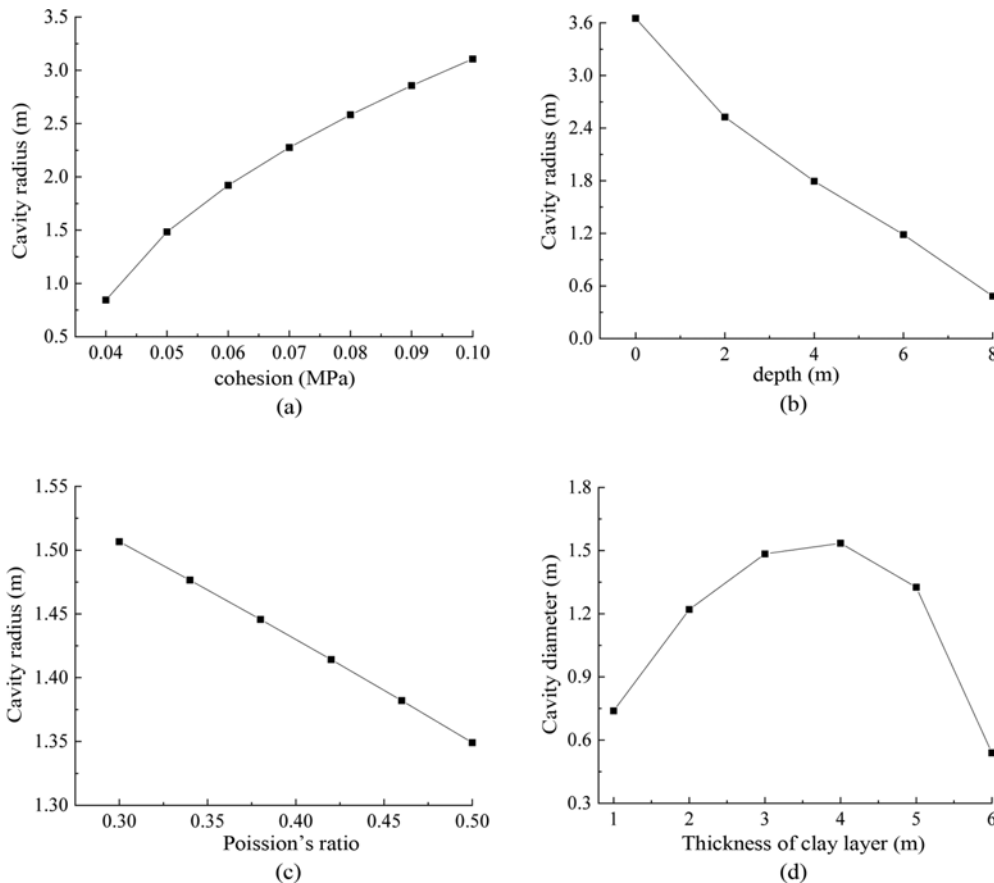


Fig. 5. Relationship between Cavity Radius and Each Influential Factor: (a) Relationship between Cavity Radius and Cohesion, (b) Relationship between Cavity Radius and Tunnel Depth, (c) Relationship between Cavity Radius and Poisson's Ratio, (d) Relationship between Cavity Radius and Clayer Thickness

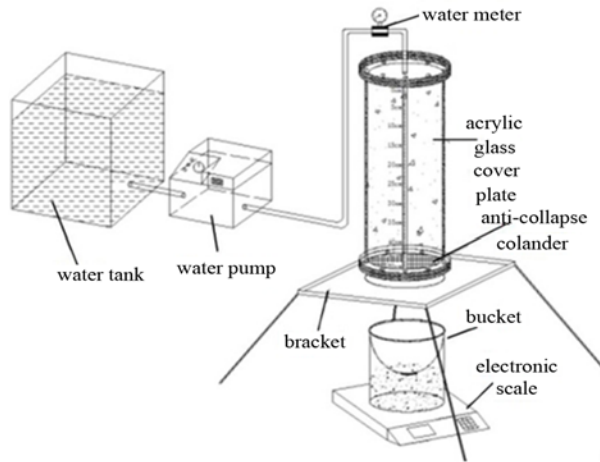


Fig. 6. Schematic Diagram of the Test Device

cohesion and thickness of clayey soil. According to Eq. (12), it is possible to analyze the variation trend of the cavity critical radius with different factors, as shown in Fig. 6. When the parameter is not discussed, the parameter is determined. The values of the parameters during the analysis are: the density of the overlying fill on the clay is  $1,750 \text{ kg/m}^3$ , its depth is 5 m. The density of clay is  $1,950 \text{ kg/m}^3$ , its friction is 13. The Poisson of clay is 0.3. The thickness of clay is 3 m. The cohesion of clay is 50 kPa. The Unified strength theory parameters is 0.6 (Yu et al., 2020).

It can be seen from Fig. 5 that:

1. The critical radius of cavity increases with the increase of clay soil cohesion. That is, the greater the clay soil strength, the more stable the clay layer, and the more particles lost needing for soil failure. When the soil cohesion is small, the soil cannot remain stable, which can explain the cause of sand collapse. When the soil particles are losing, the soil arch cannot be formed due to the lack of cohesion of the sand, and the soil cave develops rapidly and surface collapse occurs.
2. The critical radius of cavity decreases with the increase of buried depth, which shows that the greater the overlying pressure of clay soil, the more unstable the soil is.
3. The critical radius of cavity decreases with the increase of Poisson's ratio. It is well-known that the better the soil quality, the lower the Poisson's ratio. Therefore, the variation law of the critical radius of cavity with Poisson's ratio shown in Fig. 5(c) reflects the influence of clay quality on the critical radius of cavity from another perspective.
4. The critical radius of cavity first increases and then decreases with the increase of soil thickness, which can explain the formation of pressure arch. When clay soil thickness is large, the tensile stress at a certain point in the soil exceeds its tensile strength, and soil block collapse and separate from its parent body to form prototype of soil cave. With the upward development of soil cave, a naturally balanced pressure arch is formed finally, so the soil would no longer be damaged. Only when the mechanical conditions change

greatly, the pressure arch will be damaged and further drives surface collapse.

## 5. Theoretical Verification

### 5.1 Experimental Apparatus and Experimental Procedure

The self-designed visual test device for investigating the collapse process of clay layer is shown in Fig. 6. The device consists of three parts. The upper part is a water supply device, which is composed of water pipes, water pumps, and permeable plates, it could ensure the stability of constant head. The permeable plate is placed above the soil to disperse the water source and prevent it from impacting the soil; The middle part is the bearing device, which is composed of glass tube, glass cover plate, sealing ring, flange and steel plate with 5 mm diameter cavity. The lower part is composed of a movable frame and a collection device. The device can accommodate a specimen with a 500 mm length and a 150 mm diameter.

According to the measurement, the density, cohesion and friction of sand soil mixture are  $19.85 \text{ kN/m}^3$ , 16 kPa,  $22^\circ$  respectively. The sand is river sand with a density of  $19 \text{ kN/m}^3$ . The process of sample preparation was as follows:

1. Before loading the soil sample, put the steel plate with 5 mm diameter cavity into the flange, and tighten the spiral orifice of the flange, then seal the experimental with a sealing ring to prevent water loss.
2. Crush the clay and then prepare sand soil mixture proportion in proportion. Then load 50mm sand soil mixture into the glass tube and compact it, and then load 50 mm sand above the soil.
3. Place the permeable plate on the top of the sample to prevent water from impacting the soil, and connect and fix the glass cover plate and sealing ring with bolts.
4. After loading the sample, inject water at the same height as the model into the glass tube to saturate it. If the soil sample can remain stable, stand for 5 min. Then inject 5 cm high water every 2 min until the soil collapses. Keep the water

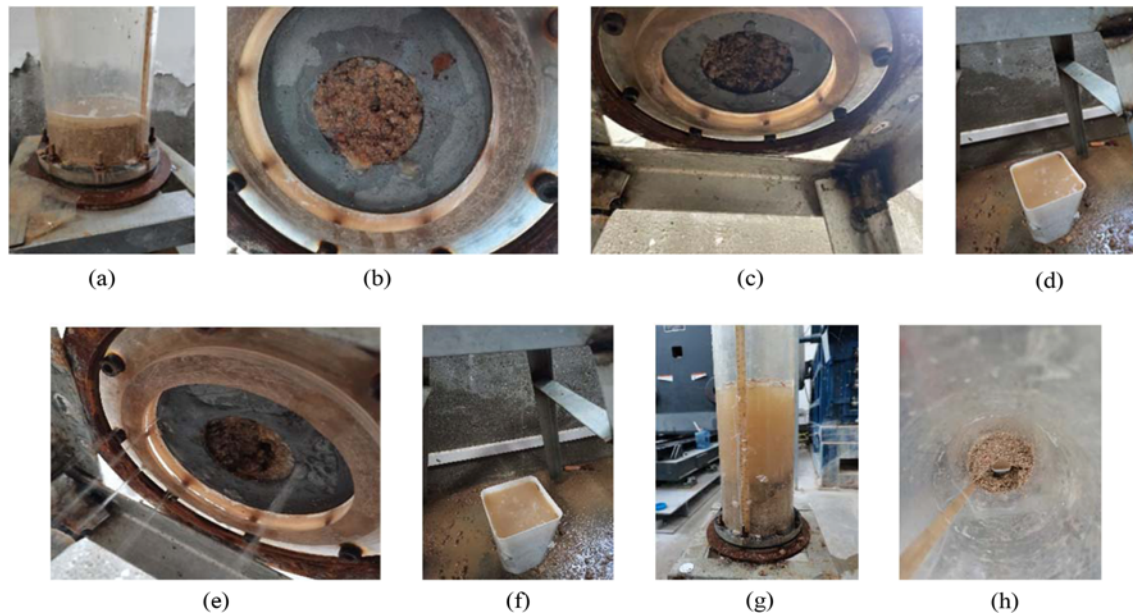


**Fig. 7.** The Process of Soil Collapses: (a) Wetting Sample, (b) Soil Falling, (c) Soil Falling, (d) Line Flow, (e) Soil Arch Formation, (f) Fascicular Flow, (g) Increase Water Head, (h) Soil Collapse

head constant during the test.

- Record the head height when the soil collapses and the phenomena during the test. Finally, clean the test device.

## 5.2 Experimental Results

The process of soil collapse is shown in Fig. 7. After the model is filled and sealed, water is injected from the top of the glass tube until the sand is submerged at the head height of 9 cm, as shown in Fig. 7(a). At this time, the soil remains stable without obvious seepage. After 2 min, add water until the head height is 11 cm. At this time, some soil falls and the sample begins to seep, but the water volume is small and dripping, as shown in Fig. 7(b). After 2 min, add water until the head height is 13 cm. At this time, some soil fall into bucket, and the water volume will increase significantly and the water flow is line shape. Which shows that a stable seepage channel is basically formed, as shown in Figs. 7(c) and 7(d). After 2 min, add water until the head height is 15 cm. At this time, some soil falls again, and the soil forms an obvious soil arch structure, as shown in Fig. 7(e). After 2 min, add water to the head height of 17 cm, the seepage channel develops further, and the water flow increases and the shape of flow is bundle, as shown in Fig. 7(f). After 2 min, add water to 21 cm water head, the soil collapse happened suddenly and a large amount of soil flows out, as shown in Fig. 7(h). During the experiment, the water flow is controlled to keep the seepage flow consistent with the water inflow as much as possible, so as to maintain the stability of the water head.

## 5.3 Data Validation

According to the theoretical Eq. (13) derived from the double shear unified strength theory in the previous section, the critical water pressure formula can be obtained:

$$P = \frac{16c_0 \cos \varphi (1+b) h^2}{(4l^2 + 2h^2 + \mu h^2)(1 + \sin \varphi)(2+b)} - (\gamma_1 h_1 + \gamma h). \quad (15)$$

The parameters are:  $\gamma = 19 \text{ kN/m}^3$ ,  $\varphi = 22^\circ$ ,  $c = 16 \text{ kPa}$ ,  $\gamma_1 = 19.85 \text{ kN/m}^3$ ,  $h_1 = 50 \text{ mm}$ ,  $h = 40 \text{ mm}$ ,  $b = 0.6$ ,  $\mu = 0.31$ ,  $l = 25 \text{ mm}$ . The critical water pressure is

$$P = \frac{16 * 0.016 * \cos 0.38 * 1.6 * 0.04 * 0.04}{(4 * 0.025^2 + 2 * 0.04^2 + 0.31 * 0.04^2)(2 + \sin 0.38)(2 + 0.6)} - (0.01985 * 0.05 + 0.019 * 0.04) = 0.018 \text{ kPa}.$$

It can be seen from the above calculation results that the critical water pressure calculated based on the unified strength theory is consistent with the model experimental value (0.021 kPa).

## 6. Discussion

Wu et al. (2018) used physical model test to study the collapse process of clay under pressure. The result show that before the water head was 145 cm, the clay layer remains stable without seepage. After that, the clay layer was damaged by seepage and clay collapse was happened. In the following 1 min, a large amount of sand leaked and ground collapse occurred. The critical cavity radius of clay collapse obtained from Wu's test and the calculation formula in this paper are 0.05 cm and 0.051 cm respectively. The error between them is 2.0%, which shows that the calculation formula could predict the critical cavity radius of clay collapses.

When a small cavity is found under the stratum, the risk of stratum collapse disaster is low at this time. However, in order to prevent the disaster, the drilling filling grouting method should be used to carry out pressure grouting on the cavity position first, deal with the cavity according to the implementation principle of

subsection and time-sharing, more complex and less grouting, and cut off the seepage channel around the cavity to prevent the further expansion of the cavity. When the cavity is large, the combination of excavation and filling grouting can be used to fill the existing cavity and strengthen the foundation.

## 7. Conclusions

Aiming at the problem of clay collapse caused by water and sand leakage, in this paper, the calculation formula of critical cavity radius for clay collapse was established by using theoretical analysis method, which is verified by indoor experimental results and existing experimental results. The conclusions are as follows:

1. The calculating formula of critical cavity radius for clay collapse induced by water and sand leakage is deduced according to the unified strength theory and clamped beam of elasticity theory. The errors of indoor experimental results and model experimental results are 2.0% and 14.2% respectively, which indicate that the calculation formula could accurately predict the critical cavity radius of clay collapse.
2. The clayey soil stability is related to depth, Poisson's ratio, cohesion and thickness of clayey soil. The critical cavity radius decreases with the increased of depth and Poisson's of clay layer. The higher the clay cohesion is, the higher the cavity radius is. The critical radius of cavity first increases and then decreases with the increased of clay thickness.

## Acknowledgments

Financial supports from Open Research Fund of State Key Laboratory of Geomechanics and Geotechnical Engineering, Institute of Rock and Soil Mechanics, Chinese Academy of Sciences, Grant NO. Z020014 is sincerely acknowledged.

## ORCID

Fan Chen  <https://orcid.org/0000-0002-5159-9338>

## References

- Chen F, Wang YC, Jiang W (2021) Numerical simulation of ground movement induced by water and sand gushing in subway through fault based on DEM-CFD. *Computer and Geotechnics* 139:104282
- Ding HJ, Huang DJ, Wang HM (2005) Analytical solution for fixed end beam subjected to uniform load. *Journal of Zhejiang University* 6A(8):779-783, DOI: 10.1007/s10483-006-1002-z
- Huang Z, Bai YC, Xu HJ (2017) A theoretical model to predict the critical hydraulic gradient for soil particle movement under two-dimensional seepage flow. *Water* 828(9):1-14, DOI: 10.3390/w9110828
- Indraratana B, Vafai F (1997) Analytical model for particle migration within base soil-filter system. *Journal of Geotechnical and Geoenvironmental Engineering* 123(6):600-600, DOI: 10.1061/(ASCE)1090-0241 (1997) 123:2(100)
- Indratna B, Nguyen VT, Rujiatkamjorn C (2011) Assessing the potential of internal erosion and suffusion of granular soils. *Journal of Geotechnical and Geoenvironmental Engineering* 137(5):550-554, DOI: 10.1061/(ASCE)GT.1943-5606.0000447
- Israr J, Indraratna B (2019) Study of critical hydraulic gradients for seepage-induced failures in granular soils. *Journal of Geotechnical and Geoenvironmental Engineering* 145(7):04019025, DOI: 10.1061/(ASCE)GT.1943-5606.0002062
- Kenney T, Lau D (1985) Internal stability of granular filters. *Canadian Geotechnical Journal* 22(2):215-225, DOI: 10.1016/0148-9062(86)91751-1
- Korff M, Mair RJ, van Tol AF, Kaalberg FJ (2011) The response of piled buildings to deep excavations. 7th international symposium on geotechnical aspects of underground construction in soft ground, May 17-19, Rome, Italy
- Li M, Fannin RJ (2012) A theoretical envelope for internal instability of cohesionless soil. *Geotechnique* 62(1):77-80, DOI: 10.1680/geot.10.T.019
- Mao CX (2005) Study on piping and filters: Part I of piping. *Rock and Soil Mechanics* 26(2):209-215, DOI: 10.16285/j.rsm.2005.02.008
- Wang ZC, Li GD (2020) Experimental study on stratigraphic subsidence induced by sand leakage in tunnel lining cracks. *Journal of Civil Engineering* 24(8):2345-2352, DOI: 10.1007/s12205-020-1958-1
- Wu ZS, Li S, Tu YL, Wang YQ (2020) Study on safety thickness theory of palm surface outburst prevention based on unified strength theory. *Chinese Journal of Underground Space and Engineering* 16(6):1705-1710 (in Chinese)
- Wu QH, Zhang W, Liu Y, Cui HD (2018) Quantifying the process of karst collapse by a physical model. *Journal of Yangtze River Scientific Research Institute* 35(3):52-58, DOI: 10.11988/ckyyb.20171079
- Xu ZL (2006) Theory of elasticity. Higher Education Press, Beijing, China, 37-46
- Yang J, Yin ZY, Zhang DM (2018) A coupled hydro-mechanical modeling of tunnel leakage in sand layer. 4th GeoShanghai international conference on tunneling and underground construction, May 27-30, Shanghai, China
- Yu MH, Wu XX, Shi J, Zhou GG (2020) A new strategy for determining failure criteria of soil. *Journal of Xi'an Jiaotong University* 54(8):1-10, DOI: 10.7652/xjtuxb202008001
- Zheng G, Dai X, Diao Y, Zeng CF (2016) Experimental and simplified model study of the development of ground settlement under hazards induced by loss of groundwater and sand. *Natural Hazards* 82:1869-1893, DOI: 10.1007/s11069-016-2275-3
- Zhong Z, Yu T (2007) Analytical solution of a cantilever functionally graded beam. *Composites Science and Technology* 67(3-4):481-488, DOI: 10.1016/j.compscitech.2006.08.023